



DNA replication studies of *N*-nitroso compound-induced O^6 -alkyl-2'-deoxyguanosine lesions in *Escherichia coli*

Received for publication, December 29, 2018, and in revised form, January 16, 2019. Published, Papers in Press, January 17, 2019, DOI 10.1074/jbc.RA118.007358

Pengcheng Wang^{‡§}, Jiapeng Leng[‡], and Yinsheng Wang^{‡#1}

From the [‡]Department of Chemistry, University of California, Riverside, California 92521-0403 and the [§]Institute of Surface Analysis and Chemical Biology, University of Jinan, Jinan, Shandong 250022, China

Edited by Patrick Sung

N-Nitroso compounds (NOCs) are common DNA-alkylating agents, are abundantly present in food and tobacco, and can also be generated endogenously. Metabolic activation of some NOCs can give rise to carboxymethylation and pyridyloxobutyl- or pyridylhydroxybutylation of DNA, which are known to be carcinogenic and can lead to gastrointestinal and lung cancer, respectively. Herein, using the competitive replication and adduct bypass (CRAB) assay, along with MS- and NMR-based approaches, we assessed the cytotoxic and mutagenic properties of three O^6 -alkyl-2'-deoxyguanosine (O^6 -alkyl-dG) adducts, *i.e.* O^6 -pyridyloxobutyl-dG (O^6 -POB-dG) and O^6 -pyridylhydroxybutyl-dG (O^6 -PHB-dG), derived from tobacco-specific nitrosamines, and O^6 -carboxymethyl-dG (O^6 -CM-dG), induced by endogenous *N*-nitroso compounds. We also investigated two neutral analogs of O^6 -CM-dG, *i.e.* O^6 -aminocarbonylmethyl-dG (O^6 -ACM-dG) and O^6 -hydroxyethyl-dG (O^6 -HOEt-dG). We found that, in *Escherichia coli* cells, these lesions mildly (O^6 -POB-dG), moderately (O^6 -PHB-dG), or strongly (O^6 -CM-dG, O^6 -ACM-dG, and O^6 -HOEt-dG) impede DNA replication. The strong blockage effects of the last three lesions were attributable to the presence of hydrogen-bonding donor(s) located on the alkyl functionality of these lesions. Except for O^6 -POB-dG, which also induced a low frequency of G → T transversions, all other lesions exclusively stimulated G → A transitions. SOS-induced DNA polymerases played redundant roles in bypassing all the O^6 -alkyl-dG lesions investigated. DNA polymerase IV (Pol IV) and Pol V, however, were uniquely required for inducing the G → A transition for O^6 -CM-dG exposure. Together, our study expands our knowledge about the recognition of important NOC-derived O^6 -alkyl-dG lesions by the *E. coli* DNA replication machinery.

Environmental exposure and endogenous metabolism can give rise to a variety of DNA adducts (1). *N*-Nitroso compounds (NOCs),² a common type of alkylating agents, are

capable of inducing cancer in ~40 different animal species, including higher primates, and are carcinogenic in multiple organs in animals (2). Humans are exposed to NOCs through dietary consumption, tobacco smoking, and endogenous metabolism (3, 4). In this vein, two potential types of carcinogenic adducts formed from NOC exposure are of emerging concern, *i.e.* the pyridyloxobutyl (POB) and pyridylhydroxybutyl (PHB) adducts derived from tobacco-specific *N*-nitrosamines and carboxymethyl adducts arising from endogenous NOCs (5, 6).

Tobacco-specific nitrosamines 4-(methylnitrosamino)-1-(3-pyridyl)-1-butanone (NNK) and *N'*-nitrosornicotine (NNN) are well-documented rodent carcinogens and classified as group I carcinogens by the International Agency for Research on Cancer (7). Metabolic activation of NNK and NNN via cytochrome P450 enzymes can produce reactive intermediates that can react with DNA to yield POB and/or PHB adducts along with other DNA lesions, which may induce mutations during DNA replication (5, 8–15). Another type of extensively investigated promutagenic lesions, carboxymethyl (CM) adducts, can be induced in DNA through metabolic activation of endogenous NOCs, *e.g.* *N*-nitroso bile acid conjugate or *N*-nitrosoglycine (16–18). It was suggested that the mutations in the *TP53* gene found in gastrointestinal cancer emanate from carboxymethylation rather than methylation of DNA elicited by NOCs (19).

Previous studies have led to the identification and quantification of a series of POB and PHB derivatives on nucleobases in DNA. O^2 -POB-dT, O^2 -PHB-dT, *N7*-POB-guanine, *N7*-PHB-guanine, O^6 -POB-dG, O^6 -PHB-dG, N^6 -POB-dA, and N^6 -PHB-dA were detected in lung and liver tissues of NNK-treated rats (8, 9, 13, 14); O^2 -POB-dT, O^6 -POB-dG, *N7*-POB-guanine, and O^2 -POB-cytosine were found in esophageal tissues of rats treated with NNN (10, 20). In addition, it was reported that appreciable levels of O^4 -POB-dT along with the above-mentioned O^2 -POB-dT and O^6 -POB-dG could be formed in cultured mammalian cells upon exposure to 4-(acetoxymethylnitrosamino)-1-(3-pyridyl)-1-butanone, a model pyridyloxobutylating agent (21, 22). Carboxymethylated DNA lesions, such as N^6 -CM-dA, *N3*-CM-dT, O^4 -CM-dT, O^6 -CM-dG, and N^4 -CM-dC were also identified *in vitro* (16, 17, 23, 24). Furthermore, O^6 -CM-dG could be induced in cultured human cells upon treatment with azaser-

This work was supported by National Institutes of Health Grant R01 ES025121. The authors declare that they have no conflicts of interest with the contents of this article. The content is solely the responsibility of the authors and does not necessarily represent the official views of the National Institutes of Health.

This article contains Scheme S1 and Figs. S1–S14.

¹ To whom correspondence should be addressed. Tel.: 951-827-2700; Fax: 951-827-4713; E-mail: Yinsheng.Wang@ucr.edu.

² The abbreviations used are: NOC, *N*-nitroso compound; CRAB, competitive replication and adduct bypass; POB, pyridyloxobutyl; PHB, pyridylhydroxybutyl; NNK, 4-(methylnitrosamino)-1-(3-pyridyl)-1-butanone; NNN, *N'*-ni-

tronsornicotine; CM, carboxymethyl; Pol, polymerase; ESI, electrospray ionization; ODN, oligodeoxyribonucleotide; PNK, polynucleotide kinase.

Replication studies of NOC-induced O⁶-alkylguanine lesions

ine, a pancreatic carcinogen that can be converted to diazoacetate by cellular esterases (25).

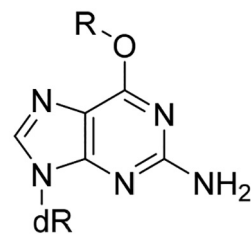
Multiple lines of evidence suggested that the O⁶ position of 2'-deoxyguanosine is the most facile exocyclic atom to be alkylated on nucleobases (26), and the resulting lesions alter the hydrogen bonding property of the guanine base (6, 27–30). In this vein, O⁶-methyl-dG (O⁶-Me-dG) and O⁶-POB-dG have been implicated in lung tumorigenesis mediated by NNK (12, 31–33), and O⁶-CM-dG may contribute to the mutations found in *TP53* tumor suppressor gene of human gastrointestinal tumors (19) and is correlated with colorectal cancer (6). Thus, it is important to understand how the O⁶-alkyl-2'-deoxyguanosine (O⁶-alkyl-dG) lesions derived from the above-mentioned NOCs affect the efficiency and fidelity of DNA replication.

Several replication studies have been performed to assess the impact of O⁶-POB-dG and O⁶-CM-dG lesions on the flow of genetic information. O⁶-POB-dG was found to be highly mutagenic, and it induces exclusively G → A transition in *Escherichia coli*, whereas it elicits both G → A transition and G → T transversion in mammalian cells (15, 33, 34). In addition, multiple translesion synthesis DNA polymerases, particularly Pol η, were found to be involved in the efficient bypass of O⁶-POB-dG (15), which is consistent with *in vitro* results showing that Pol η exhibits much higher efficiency in bypassing O⁶-POB-dG than Pol ι, Pol κ, and Rev1 (35, 36). O⁶-CM-dG is able to form Watson–Crick-type bp with thymidine, thereby inducing G → A transition mutation (37). In mammalian cells, Pol κ and Pol ζ are required for the efficient bypass of this lesion, and only G → A transition was observed (38). However, it remains unknown how O⁶-PHB-dG compromises the efficiency and accuracy of DNA replication.

Herein, we incorporated O⁶-POB-dG, O⁶-PHB-dG, O⁶-CM-dG, and its two analogs, *i.e.* O⁶-aminocarbonylmethyl-dG (O⁶-AMC-dG) and O⁶-hydroxyethyl-dG (O⁶-HOEt-dG), into single-stranded plasmids and examined how these lesions impede DNA replication and elicit mutation(s) in *E. coli* cells. We also explored the roles of SOS-induced DNA polymerases in bypassing these lesions.

Results

The primary objective of this project was to elucidate how the O⁶-substituted guanine lesions arising from tobacco-derived and endogenous NOCs (Fig. 1) compromise the efficiency and fidelity of DNA replication in *E. coli* cells. To this end, ODNs harboring a series of O⁶-alkyl-dG lesions at a specific site were synthesized and confirmed by ESI-MS and MS/MS analyses (Fig. 2 and Figs. S1–S7). A previously described CRAB assay (Fig. 3 and Fig. S8) was employed to determine the impacts of these lesions on DNA replication in *E. coli* cells and to determine how replication across these lesions is influenced by SOS-induced DNA polymerases (39, 40). After cellular replication, the region of interest in the progeny genomes was amplified by PCR, the ensuing products were digested with two restriction endonucleases, *i.e.* BbSI and MluCI, and the restriction fragments were analyzed by LC-MS/MS and native PAGE (Fig. 4 and Figs. S9–S14).



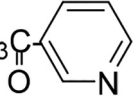
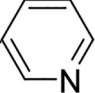
R = -CH ₂ CH ₂ OH	O ⁶ -HOEt-dG
-CH ₂ COOH	O ⁶ -CM-dG
-CH ₂ CONH ₂	O ⁶ -ACM-dG
-(CH ₂) ₃ C(=O)- 	O ⁶ -POB-dG
-(CH ₂) ₃ CH(OH)- 	O ⁶ -PHB-dG

Figure 1. The O⁶-substituted dG lesions considered in this study. dR represents 2-deoxyribose.

The impacts of O⁶-POB-dG and O⁶-PHB-dG on the efficiency and fidelity of DNA replication

Our results from PAGE and LC-MS/MS analyses revealed the lack of insertion or deletion mutations (Fig. 4 and Fig. S9–S14). Hence, we calculated the bypass efficiencies of O⁶-POB-dG and O⁶-PHB-dG from the ratio of the 10-mer products emanating from lesion and control genomes, over the 13-mer product, generated from the competitor plasmid (Fig. 4 and Figs. S11–S14), by taking into account the molar ratios of the lesion and control over the competitor genomes employed at the initial transfection. It turned out that these two lesions were moderate impediments to DNA replication in WT AB1157 cells, with O⁶-PHB-dG exerting a stronger blockage effect (Fig. 5A).

The roles of SOS-induced DNA polymerases in bypassing the O⁶-POB-dG and O⁶-PHB-dG were also investigated by performing the assay in *E. coli* strains deficient in Pol II, Pol IV, Pol V, or all three in combination. It turned out that a substantial diminution in bypass efficiency was observed only when all three SOS-induced DNA polymerases were depleted, which is consistent with the observations made previously for other O⁶-alkyl-dG lesions (30). No significant differences were observed for the bypass efficiencies of O⁶-POB-dG and O⁶-PHB-dG lesions in AB1157 cells and the isogenic cells with a single depletion of any of the three polymerases (Fig. 5A). This result supports that the three SOS-induced DNA polymerases assume somewhat redundant roles in bypassing O⁶-POB-dG and O⁶-PHB-dG.

The native PAGE analysis also facilitated the quantification of the mutation frequencies of O⁶-POB-dG and O⁶-PHB-dG. In agreement with previous findings (30), the major type of mutation was G → A transition for both O⁶-POB-dG and O⁶-PHB-dG in all *E. coli* strains (Fig. 5B). A low frequency of G → T transversion, however, was also detected for

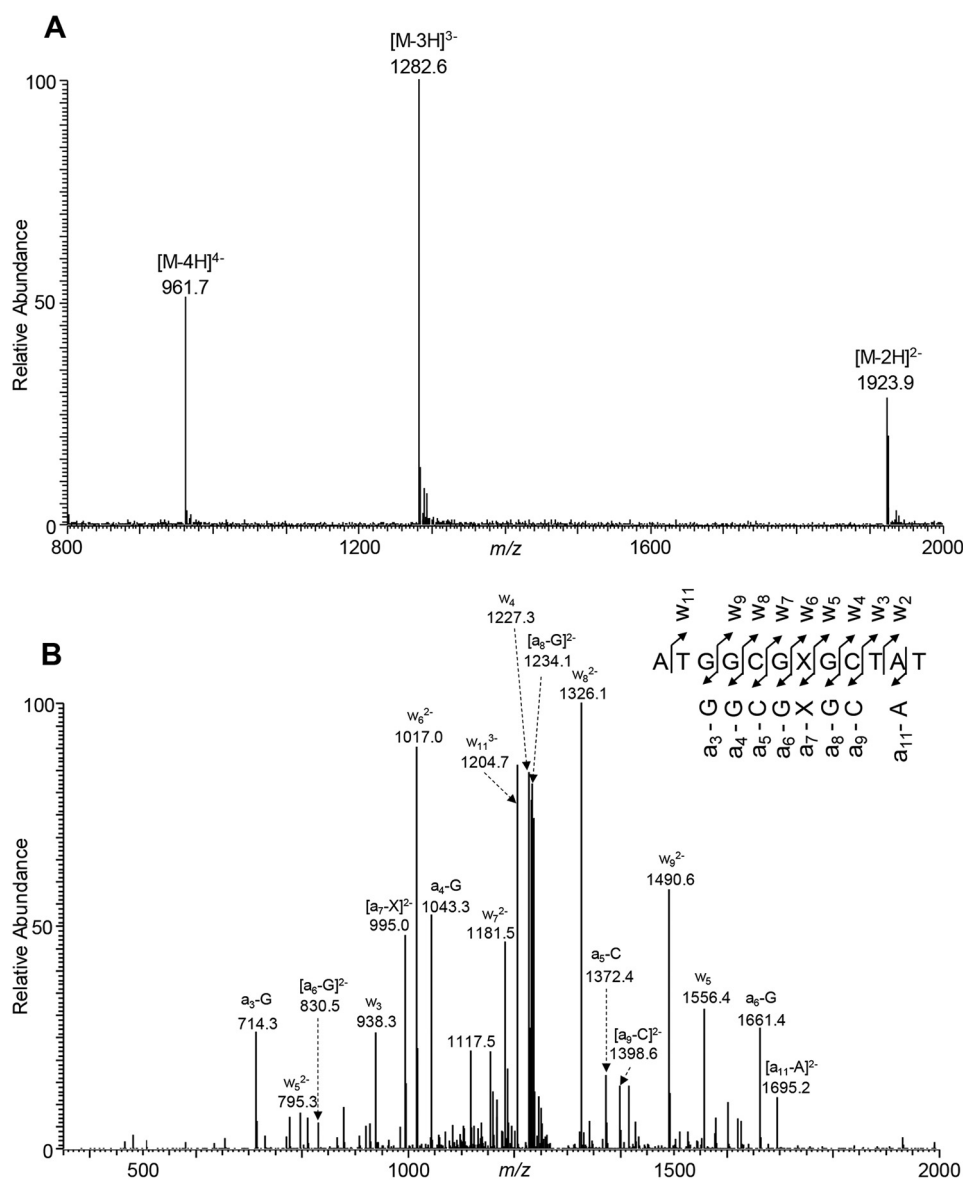


Figure 2. ESI-MS and MS/MS characterizations of d(ATGGCGXGCTAT), where X = O^6 -PHB-dG. A, negative-ion ESI-MS. B, product-ion spectrum of the [M - 3H]³⁻ ion (m/z 1282.6).

O^6 -POB-dG (Fig. 5C), which differs from the previously reported results (34). We also found that the frequencies of the mutations conferred by O^6 -POB-dG and O^6 -PHB-dG were not affected by depletion of any of the three SOS-induced DNA polymerases, individually or all three together (Fig. 5, B and C). This result underscores that the observed mutations can be attributed to the intrinsic hydrogen-bonding properties of the O^6 -substituted guanine, which preferentially forms bp with thymine.

The impacts of O^6 -CM-dG, O^6 -ACM-dG, and O^6 -HOEt-dG on the efficiency and fidelity of DNA replication

Different from O^6 -POB-dG, O^6 -PHB-dG, and the previously reported O^6 -alkyl-dG lesions (30), O^6 -CM-dG displayed strong blockage to DNA replication machinery in WT AB1157 cells, as manifested by a ~10% bypass efficiency (Fig. 6A). Interestingly, this bypass efficiency was augmented by almost 2-fold upon SOS induction.

The unique strong blockage effect of O^6 -CM-dG on cellular DNA replication prompted us to ask whether the negative charge located on the carboxymethyl functionality modulates the bypass efficiency of the lesion. To test this, we synthesized two other O^6 -modified derivatives with the carboxymethyl moiety being replaced with an aminocarbonylmethyl or hydroxyethyl group (Fig. 1), which are neutral under cellular pH. It turned out that O^6 -ACM-dG and O^6 -HOEt-dG also exhibited very low bypass efficiencies (Fig. 6A). Hence, we attribute the low bypass efficiencies of O^6 -CM-dG and the other two derivatives to the terminal hydrogen bond donor (*i.e.* hydroxyl or amino group) conjugated with the alkyl functionality adducted to the O^6 position of guanine. It is worth noting that, similar to what we observed for O^6 -POB-dG and O^6 -PHB-dG, the bypass efficiencies of these three lesions were not affected by individual depletion of Pol II, Pol IV, or Pol V (Fig. 6A).

Replication studies of NOC-induced O^6 -alkylguanine lesions

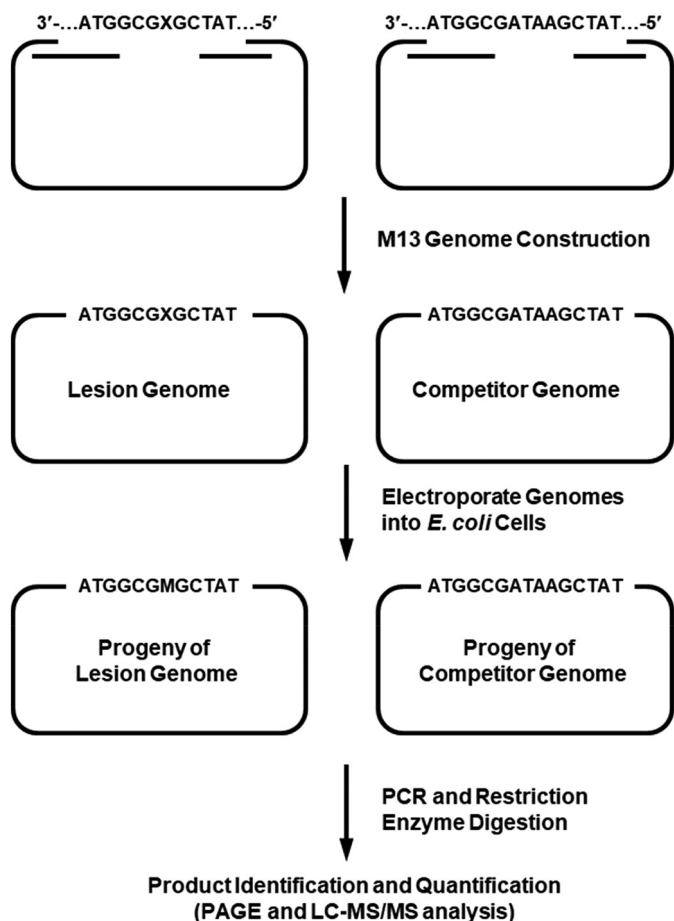


Figure 3. A schematic diagram illustrating the experimental procedures of the modified CRAB assay.

The mutation frequencies were also quantified, where only $G \rightarrow A$ transition was observed for all three lesions in all *E. coli* strains studied (Fig. 6B). In addition, the frequencies of $G \rightarrow A$ transition for O^6 -ACM-dG and O^6 -HOEt-dG were not influenced by depletion of any of the SOS-induced DNA polymerases, alone or all three in combination. However, O^6 -CM-dG distinguishes from other lesions, where Pol V and, to a lesser extent, Pol IV were required for the $G \rightarrow A$ transition mutation. Thus, the negative charge possessed by the carboxymethyl functionality affects the involvement of SOS-induced DNA polymerases in dTMP misincorporation opposite the lesion (Fig. 6B).

Discussion

There is established evidence for the association of tobacco use with lung cancer, and lung cancer is the second most common type of cancer diagnosed in both men and women (41). In addition, red meat-containing diet, especially processed meat, are risk factors for gastrointestinal cancer, which constitutes one of the leading causes of cancer-related deaths worldwide (42, 43). Previous studies revealed that the POB, PHB, and CM adducts of DNA derived from the NOCs in tobacco and red meat may be important factors contributing to the development of lung and colorectal cancer.

We investigated the replicative bypass of O^6 -POB-dG, O^6 -PHB-dG, and O^6 -CM-dG in *E. coli* cells, where O^6 -PHB-dG

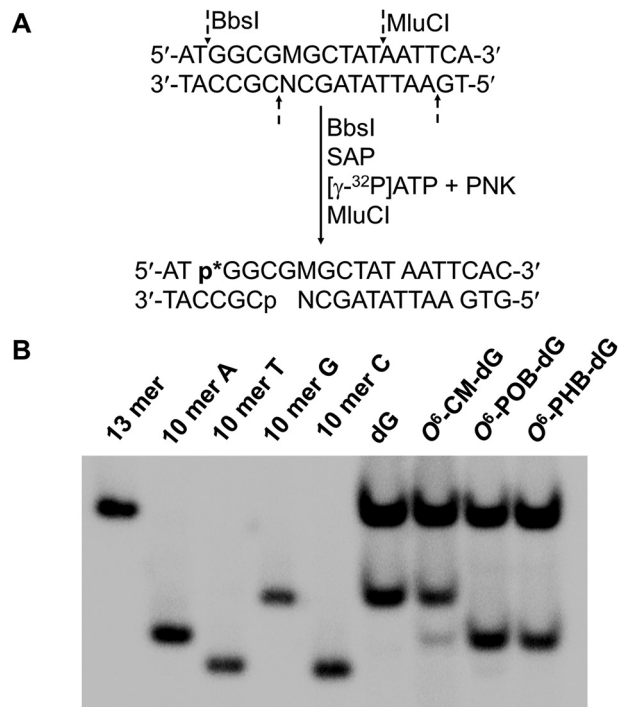


Figure 4. Native PAGE (30%) for monitoring the bypass efficiencies and mutation frequencies of O^6 -CM-dG, O^6 -POB-dG, and O^6 -PHB-dG in SOS-induced WT AB1157 *E. coli* cells. *A*, sequential restriction enzyme digestion and selective radiolabeling of the strand initially bearing the lesion. *SAP* and *PNK* designate shrimp alkaline phosphatase and T4 polynucleotide kinase, respectively. *B*, gel image showing 10-mer radiolabeled restriction fragments released from the original lesion-containing strand of the PCR products of the progeny of the control or lesion-carrying genome, where 10-mer A, 10-mer C, 10-mer G, and 10-mer T represent the 5'- ^{32}P -labeled standard ODNs 5'-GGCGMGCTAT-3', where *M* is A, C, G, and T, respectively. Both O^6 -POB-dG and O^6 -PHB-dG are highly mutagenic and mainly induce $G \rightarrow A$ transition (10-mer A), although a low rate of $G \rightarrow T$ mutation (10-mer T) was also observed for O^6 -POB-dG. O^6 -CM-dG induced a much lower frequency of $G \rightarrow A$ mutation. The 13-mer radiolabeled band is the corresponding fragment liberated from the PCR product of the competitor genome.

was studied here for the first time. Our results revealed several novel findings. First, we observed that O^6 -POB-dG and O^6 -PHB-dG were slight and moderate impediments to DNA replication, respectively, whereas replication past O^6 -CM-dG was strongly inhibited (Figs. 5A and 6A). Second, we found that the three SOS-induced DNA polymerases, *i.e.* Pol II, Pol IV, and Pol V, assume redundant roles in bypassing the three O^6 -alkyl-dG lesions (Fig. 5A and 4A). Third, our results demonstrated that these lesions induce $G \rightarrow A$ transition exclusively, except that $G \rightarrow T$ transversion was also observed for O^6 -POB-dG (Fig. 5, B and C, and 6B). Fourth, we revealed that the mutation frequencies of O^6 -POB-dG and O^6 -PHB-dG were not affected by depletion of Pol II, Pol IV, Pol V, or all three polymerases; however, Pol V and, to a lesser extent, Pol IV play important roles in eliciting $G \rightarrow A$ transition for O^6 -CM-dG (Fig. 5, B and C, and 6B).

Previously, it was found that O^6 -alkyl-dG lesions, with the alkyl group ranging from methyl to *sec*-butyl, do not inhibit DNA replication in *E. coli* cells and the three SOS-induced DNA polymerases play somewhat redundant roles in bypassing these lesions (30). Here, we found that O^6 -POB-dG, O^6 -PHB-dG, and O^6 -CM-dG exhibited slight, moderate, and strong blockage to DNA replication, respectively.

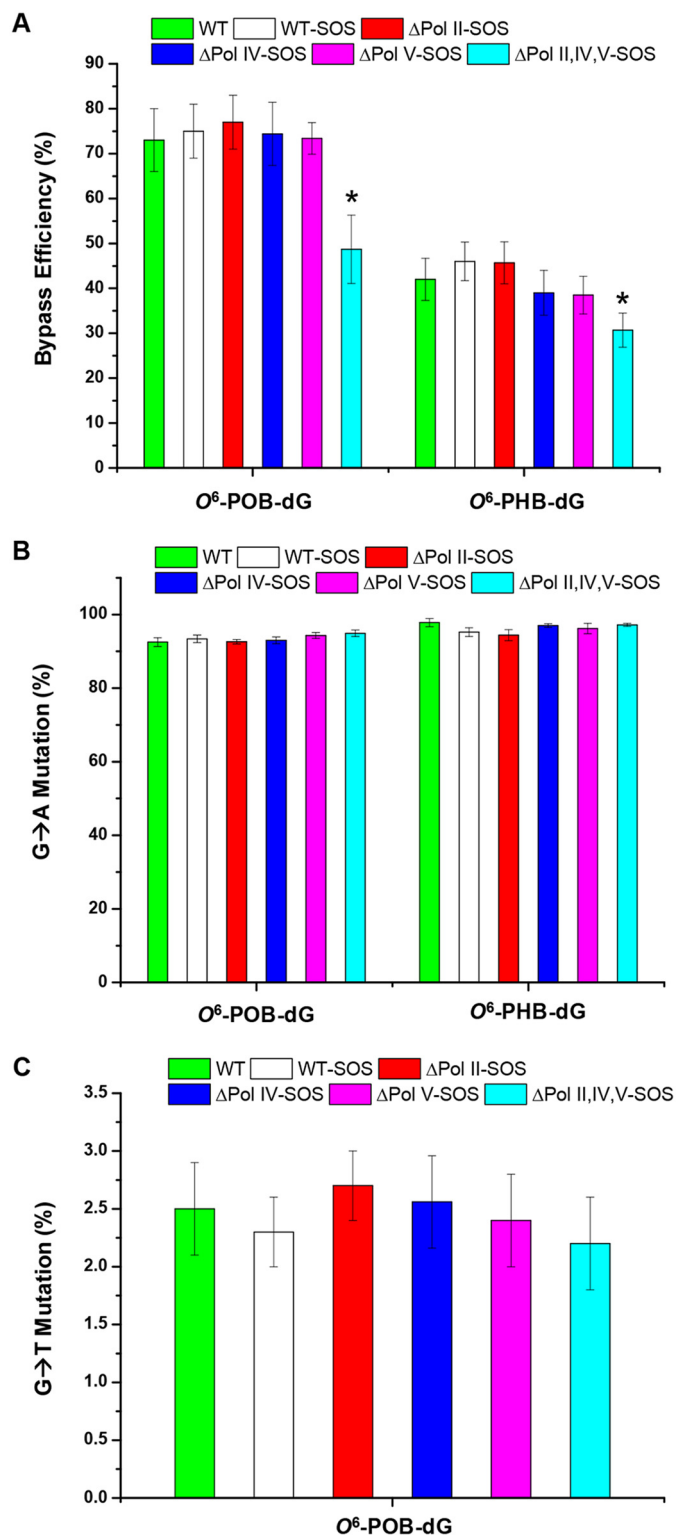


Figure 5. The bypass efficiencies (A) and G → A (B) or G → T (C) mutation frequencies of O^6 -POB-dG and O^6 -PHB-dG in AB1157 *E. coli* strains that are proficient in translesion synthesis or deficient in Pol II, Pol IV, and Pol V, alone or all three together. The data represent the means and standard deviation of results from three independent replication experiments. The p values were calculated using two-tailed, unpaired Student's t test. *, $0.01 < p < 0.05$.

We further explored the mechanism underlying the very low bypass efficiency of O^6 -CM-dG. On the grounds that the carboxylic acid functionality in O^6 -CM-dG would be deproto-

nated and carry a negative charge in cellular pH, we initially hypothesized that the negative charge may contribute to the diminished replicative bypass of O^6 -CM-dG. To test that hypothesis, we assessed how two neutral analogs of O^6 -CM-dG, *i.e.* O^6 -ACM-dG and O^6 -HOEt-dG, impede DNA replication. It turned out that the latter two lesions strongly block DNA replication, with the bypass efficiency of O^6 -ACM-dG being merely ~2% (Fig. 6A). These results unveiled that the poor replicative bypass of O^6 -CM-dG is not due to the presence of a negative charge situated on the carboxymethyl group of the lesion. Instead a hydrogen bond-donating hydroxyl or amino group at the terminus of the alkyl chain significantly impedes the replicative bypass (Fig. 6A), which is perhaps due to the disruption of the interaction between the lesions and the active site of polymerases (44, 45). Similar mechanism is likely at play for the substantially lower bypass efficiency of O^6 -PHB-dG than O^6 -POB-dG (Fig. 5A). However, future structural studies are required for understanding the detailed molecular mechanism underlying the strong blockage effects of these lesions. In addition, it should be noted that, consistent with the previously reported results for simple O^6 -alkyl-dG lesions (30), genetic ablation of Pol II, Pol IV, or Pol V did not confer any significant difference in replicative bypass of any of the five O^6 -alkyl-dG lesions examined in the present study (Fig. 6A).

It was previously shown that in *E. coli* cells, simple aliphatic O^6 -alkyl-dG lesions only induce G → A transition, which also holds true for the complex O^6 -POB-dG lesion (30, 34). In mammalian cells, the primary type of mutation elicited by O^6 -alkyl-dG lesions is the G → A transition, although a low frequency of G → T transversion was also detected for O^6 -POB-dG (15, 34). In line with these previous observations, the five lesions examined in the present study directed primarily G → A transition (Figs. 5, B and C, and 6B). However, different from the results obtained from replication experiments employing colony picking and Sanger sequencing analysis (34), a low frequency of G → T transversion (~2%) was also observed for O^6 -POB-dG in *E. coli* cells (Fig. 5C). This result underscores that the modified CRAB assay is more sensitive, thereby allowing for the detection of low frequencies of mutations better than the previously reported method (34).

The mutation frequencies for O^6 -POB-dG, O^6 -PHB-dG, O^6 -ACM-dG, and O^6 -HOEt-dG were not modulated by SOS-induced DNA polymerases, where genetic ablation of Pol II, Pol IV, and Pol V, alone or all three in conjunction, did not confer any appreciable changes in frequencies of G → A transition, or, for O^6 -POB-dG, G → T transversion mutation (Figs. 5, B and C, and 6B), suggesting that the mutagenic properties of the O^6 -alkyl-dG lesions are independent of the size or shape of the alkyl groups and arise from the intrinsic chemical property of the lesions, *i.e.* their capabilities in hydrogen bonding and in mispairing with thymidine.

Intriguingly, different from the above four O^6 -alkyl-dG lesions, two SOS-induced DNA polymerases, *i.e.* Pol IV and Pol V, play important roles in inducing G → A transition for O^6 -CM-dG (Fig. 6B), and the frequency of this mutation was increased by 2-fold upon SOS induction, substantiating that the mutagenic properties of O^6 -alkyl-dG lesions can be modulated by the negative charge situated on the O^6 position of guanine.

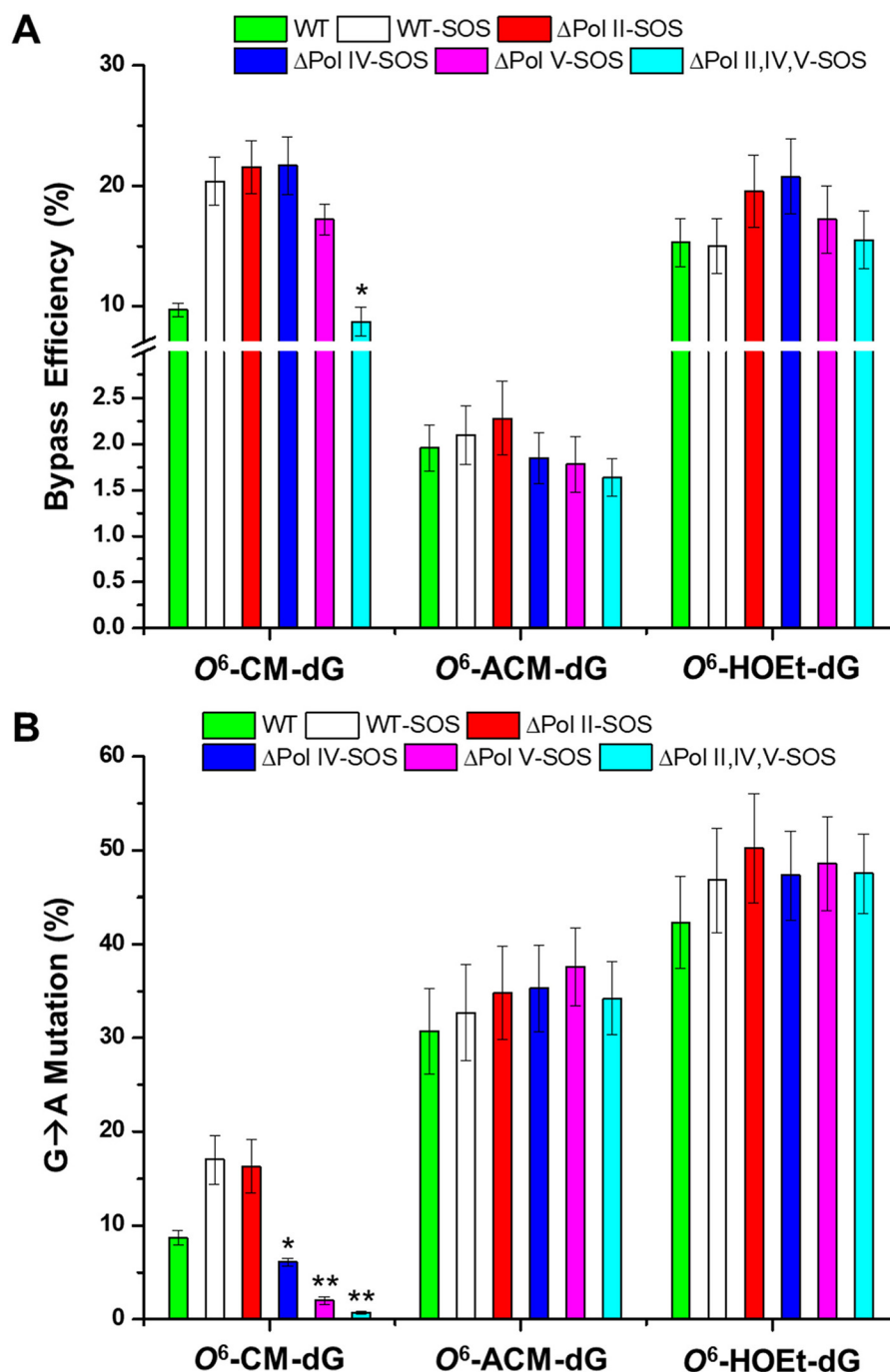


Figure 6. The bypass efficiencies (A) and mutation frequencies (B) of O⁶-CM-dG, O⁶-HOEt-dG, and O⁶-ACM-dG in AB1157 *E. coli* strains that are proficient in translesion synthesis or deficient in Pol II, Pol IV, and Pol V, alone or all three in combination. The data represent the means and standard deviation of results from three independent replication experiments. The *p* values were calculated using two-tailed, unpaired Student's *t* test. *, 0.01 ≤ *p* < 0.05; **, 0.001 ≤ *p* < 0.01.

For all the neutral substituents, from simple methyl to complex POB or PHB, the nucleotide insertion opposite the lesion was not affected by SOS-induced DNA polymerases. The mutagenic nucleotide insertion opposite the negatively charged O⁶-CM-dG is, however, influenced by Pol IV and Pol V (Fig. 6B). It should be noted that, in non-SOS-induced *E. coli* cells, Pol V could not be detected biochemically, and its expression level would increase by ~100-fold upon SOS induction (46–48). In addition, Pol V plays crucial roles in replicative bypass of multiple lesions, such as oxidized guanine lesions and O²-alky-

lated thymidine lesions, where it promotes error-prone replication under many circumstances (40, 48, 49).

It is worth comparing the findings made in *E. coli* cells with previously reported results in mammalian cells. It was found that O⁶-POB-dG directed primarily the G → A transition with a low frequency of G → T transversion in HEK293T cells (15), which is in agreement with what we observed in *E. coli* cells. However, translesion synthesis polymerases, *i.e.* Pol η, Pol ι, Pol κ, and Pol ζ, are all required for the efficient bypass of this lesion in human cells (15). Likewise, O⁶-CM-dG confers exclusively

G → A transition in HEK293T cells, and it moderately impedes DNA replication (with a 38% bypass efficiency), where Pol κ and Pol ζ are involved in bypassing this lesion (38). On the other hand, O⁶-CM-dG displays only a ~10% bypass efficiency in WT *E. coli* cells, and the three SOS-induced polymerases play redundant roles in bypassing this lesion.

It is also important to compare the results obtained for the major-groove O⁶-alkyl-dG lesions with previous findings made for minor-groove N²-alkyl-dG lesions. In this vein, the minor-groove N²-alkyl-dG lesions exert moderate blocking effects on DNA replication (50). For instance, a site-specifically incorporated N²-(1-carboxyethyl)-2'-deoxyguanosine (N²-CE-dG) was not a strong impediment to DNA replication in WT AB1157 cells, with the bypass efficiencies of S- and R-N²-CE-dG being ~80 and ~40%, respectively (50). However, the efficient and accurate replication across N²-alkyl-dG lesions in *E. coli* requires Pol IV, and their accurate bypass in human cells necessitates both Pol κ (an ortholog of Pol IV) and Pol ι (50–54). These differences perhaps can be attributed to the differences in replication machineries of *E. coli* and human cells.

In summary, our shuttle vector-based study on a group of NOC-derived O⁶-alkyl-dG lesions provided important and novel insights into the impact of carboxymethyl and pyridyl-oxobutyl/pyridylhydroxybutyl DNA lesions on the efficiency and fidelity of DNA replication in cells. Our results revealed strong miscoding potentials of the O⁶-POB-dG and O⁶-PHB-dG derived from tobacco-specific nitrosamines. In addition, our results revealed the hydrogen-bonding donor and negative charge situated on the O⁶-alkyl group as important determinants of DNA replication in *E. coli* cells. It will be important to assess how these O⁶-alkyl-dG lesions compromise DNA replication and transcription in mammalian cells in the future.

Experimental procedures

All chemicals, unless otherwise specified, were from Sigma-Aldrich or Thermo Fisher Scientific. 1,1,1,3,3,3-Hexafluoro-2-propanol was obtained from Oakwood Products, Inc. (West Columbia, SC). Reagents for solid-phase DNA synthesis were purchased from Glen Research Co. (Sterling, VA) and unmodified oligodeoxyribonucleotides (ODNs) were from Integrated DNA Technologies (Coralville, IA). All enzymes were obtained from New England Biolabs (Ipswich, MA), and [γ -³²P]ATP was purchased from PerkinElmer Life Sciences.

M13mp7(L2) and WT AB1157 *E. coli* strain were kindly provided by Prof. John M. Essigmann. Polymerase-deficient AB1157 strains (Δ pol BI::spec (Pol II-deficient), Δ dinB (Pol IV-deficient), Δ umuC::kan (Pol V-deficient), Δ umuC::kan Δ dinB (Pol IV, Pol V double knockout), and Δ pol BI::spec Δ dinB Δ umuC::kan (Pol II, Pol IV, Pol V triple knockout)) were generously provided by Prof. Graham C. Walker (49).

MS and NMR

ESI-MS and MS/MS experiments were carried out on an LCQ Deca XP ion-trap mass spectrometer (Thermo Fisher Scientific). A mixture of acetonitrile and water (50:50, v/v) was used as the solvent for electrospray. The spray voltage was 3.0 kV, and the temperature of the ion transport tube was maintained at 275 °C. High-resolution mass spectra were acquired

on an Agilent 6510 Q-TOF LC/MS mass spectrometer (Agilent Technologies, Palo Alto, CA) equipped with an ESI source. ¹H and ³¹P NMR spectra were recorded at 400 and 80 MHz on an Avance NEO 400 NMR spectrometer (Bruker, Billerica, MA) at 25 °C, respectively.

Preparation of the lesion-carrying ODNs

The 12-mer lesion-containing ODNs, 5'-ATGGCGXGC-TAT-3' (X = O⁶-alkyl-dG; Fig. 1), were synthesized via automated solid-phase DNA synthesis on a Beckman Oligo 1000M DNA synthesizer (Fullerton, CA). Commercially available ultramild phosphoramidites were employed for the incorporation of unmodified nucleotides (Glen Research Inc., Sterling, VA) following the standard ODN assembly protocol. The phosphoramidite building block for O⁶-HOEt-dG was prepared following published procedures (Scheme S1) (30, 55, 56); the yields and spectroscopic characterizations of the synthetic products are provided in the supporting materials (Figs. S1–S4).

O⁶-Aminocarbonylmethyl-dG (O⁶-AMC-dG)-containing ODN was deprotected by treating the solid support of O⁶-CM-dG containing ODN with concentrated ammonium hydroxide (57). All other 12-mer lesion-containing ODNs were cleaved from the solid support and deprotected with 0.25 M NaOH at room temperature overnight, and the resulting solution was subsequently neutralized with 0.5 M HCl. The O⁶-POB-dG-containing ODN was synthesized following previously published procedures (58), and the O⁶-PHB-dG-containing ODN was obtained by incubation of the O⁶-POB-dG-containing ODN with sodium borohydride (5 eq) in H₂O for 5 min in an ice-water bath.

The solvents were removed under vacuum, and the solid residues were redissolved in water and purified via reversed-phase HPLC, with the use of a Kinetex XB-C18 column (4.6 × 150 mm, 5 μ m in particle size, and 100 Å in pore size; Phenomenex Inc., Torrance, CA), as described elsewhere (39, 40). The HPLC traces for the purification of the 12-mer lesion-carrying ODNs are displayed in Fig. S5, and the mass spectrometric characterizations of the purified lesion-containing ODNs are shown in Fig. 2 and supporting Figs. S6 and S7. The purified 12-mer O⁶-alkyl-dG-containing ODNs were then ligated individually with a 10-mer ODN (5'-AGTGGAAGAC-3') with T4 DNA ligase in the presence of a template ODN, and the desired 22-mer lesion-bearing ODNs were purified using denaturing PAGE, as described previously (39, 40).

Construction of single-stranded lesion-containing and lesion-free competitor M13 genomes

The lesion-containing and lesion-free M13mp7(L2) genomes were prepared following previously reported procedures (Fig. S8) (59). Briefly, 20 pmol of single-stranded M13 genome was first linearized via digestion with 40 units of EcoRI at 23 °C for 8 h. The ensuing linearized vector was then annealed with two scaffolds: 5'-CTTCCACTCACTGAATCATGGTCATAGCTTTC-3' and 5'-AAAACGACGGCCAGTGAATTATAGC-3' (25 pmol). To the resulting mixture was subsequently added 30 pmol of the 5'-phosphorylated 22-mer O⁶-alkyl-dG-bearing ODN or the competitor ODN (25-mer, 5'-AGTGGAAGACATGGCGATAAGC-TAT-3'). The mixture was then treated with T4 DNA ligase at

Replication studies of NOC-induced O⁶-alkylguanine lesions

16 °C for 8 h. After the ligation, excess scaffolds and the unligated vector were degraded by incubating with T4 DNA polymerase (22.5 U) at 37 °C for 4 h. The desired lesion-containing and the lesion-free M13 genomes were purified from the resultant mixture using a Cycle Pure kit (Omega). The constructed lesion-containing or control genomes were normalized against the lesion-free competitor genome following published procedures to determine accurately the relative concentrations of the constructed genomes (59).

Transfection of lesion-containing and competitor M13 genomes into *E. coli* cells

The control lesion-free M13 genome was mixed with the competitor genome at a molar ratio of 1:1. The O⁶-POB-dG- and O⁶-PHB-dG- containing M13 genomes were mixed individually with the competitor genome at a molar ratio of 2:1. The O⁶-CM-dG-, O⁶-ACM-dG-, and O⁶-HOEt-dG- carrying M13 genomes were mixed with the competitor genome at a molar ratio of 5:1. The mixtures were transfected into SOS-induced, electrocompetent WT AB1157 *E. coli* cells and the isogenic *E. coli* cells that are deficient in pol II, pol IV, pol V, or all three polymerases (59). The SOS response was induced by irradiating *E. coli* cells with 254 nm light at a dose of 45 J/m², as previously described (49).

The *E. coli* cells were subsequently grown in lysogeny broth culture medium at 37 °C for 6 h. The phage was recovered from the supernatant by centrifugation at 13,000 r.p.m. for 5 min and further amplified in SCS110 *E. coli* cells to increase the progeny/lesion-genome ratio. The amplified phage was finally purified using the QIAprep Spin M13 kit (Qiagen) to obtain the ssM13 DNA template for PCR amplification.

Quantification of bypass efficiencies and mutation frequencies

A modified version of the CRAB assay was employed to assess the bypass efficiencies of the O⁶-alkyl-dG lesions *in vivo* (Fig. 3) (50, 59). The region of interest in the purified ssM13 DNA template was amplified by PCR with Phusion high-fidelity DNA polymerase (NEB) using two primers, 5'-YCAGCTATGACCATGATTCAGTGAGTGGA-3' and 5'-YTGGGTGCGGGCCTCTTCGCTATTAC-3' (where Y is an amino group). PCR amplification was conducted for 30 cycles, each of which consisted of 10 s at 98 °C, 30 s at 65 °C, and 15 s at 72 °C, with a final extension at 72 °C for 5 min.

The PCR products were then subjected to sequential restriction endonuclease digestion and native PAGE analysis for determination of bypass efficiency and mutation frequency (Fig. 4 and Figs. S11–S14). Briefly, 80 ng of the PCR products were treated with BbsI (10 units) restriction endonuclease and shrimp alkaline phosphatase (SAP, 1 unit) in 10 μl of CutSmart buffer (NEB) at 37 °C for 30 min. The SAP was deactivated by heating at 80 °C for 10 min, and the mixture was incubated with T4 polynucleotide kinase (PNK, 10 units), DTT (5 mM), and [γ -³²P]ATP at 37 °C for 30 min to radiolabel the newly released 5'-termini of the restriction fragments. After deactivation of T4 PNK via heating at 80 °C for 10 min, the resultant mixture was digested with MluCI (10 μl) at 37 °C for 30 min. Under these conditions, the 10-mer ODNs emanating from initial lesion-

situated strand were radiolabeled as d(p*GGCGMGCTAT), where M indicates A, T, G, and C, and p* designates the 5'-³²P-labeled phosphate (Fig. 4A).

The digestion was subsequently quenched with 15 μl of formamide gel-loading buffer (2×), and the labeled fragments were separated using 30% native PAGE, as previously described (Fig. 4 and Figs. S11–S14) (39, 40). The intensities of the radiolabeled DNA bands were measured using a Typhoon 9410 variable mode imager, and the bypass efficiency was derived using the following equation: bypass efficiency (%) = (lesion signal/competitor signal)/(control signal/competitor signal) × 100%, where the competitor signal was employed as the internal standard.

The mutation frequencies were determined according to previously published procedures (39, 40). As shown in Fig. 4B, the two products with M being an A or G could be well-resolved by native PAGE analysis; hence, native PAGE analysis of the initial lesion-bearing strand was sufficient for quantifying the G → A transition frequency. In addition, the G → T transversion elicited by O⁶-POB-dG was further confirmed via PAGE analysis of the strand that is complementary to the original lesion-containing strand (Fig. S14).

Identification of mutagenic products by LC-MS/MS

The PCR products were digested with 50 units of BbsI restriction endonuclease and 20 units of shrimp alkaline phosphatase in 250 μl of NEB CutSmart buffer at 37 °C for 2 h, followed by deactivation of the enzymes through heating at 80 °C for 20 min. To the mixture was added 50 units of MluCI, and the solution was incubated at 37 °C for 1 h. The resulting solution was extracted once with phenol/chloroform/isoamyl alcohol (25:24:1, v/v). The aqueous layer was subsequently dried in a SpeedVac, desalted with HPLC, and dried again. The resultant solid residues were reconstituted in 20 μl of water, and a 10-μl aliquot was injected for LC-MS/MS analysis using an Agilent Zorbax SB-C18 column (0.5 × 250 mm, 5 μm in particle size). The gradient for LC-MS/MS analysis was 5 min of 5–20% methanol followed by 35 min of 20–50% methanol in 400 mM 1,1,1,3,3,3-hexafluoro-2-propanol. The temperature for the ion-transport tube was maintained at 300 °C. The LTQ linear ion trap mass spectrometer (Thermo Electron, San Jose, CA) was set up for monitoring the fragmentation of the [M-3H]³⁻ ions of the 10-mer d(GGCGMGCTAT), where M represents A, T, C, or G. The fragment ions detected in the MS/MS were manually assigned (Figs. S9 and S10).

Author contributions—P. W. data curation; P. W. formal analysis; P. W. and J. L. investigation; P. W. methodology; P. W. writing-original draft; P. W., J. L., and Y. W. writing-review and editing; Y. W. conceptualization; Y. W. supervision; Y. W. funding acquisition.

References

1. Fu, D., Calvo, J. A., and Samson, L. D. (2012) Balancing repair and tolerance of DNA damage caused by alkylating agents. *Nat. Rev. Cancer* **12**, 104–120 [CrossRef Medline](#)
2. Bogovski, P., and Bogovski, S. (1981) Animal species in which N-nitroso compounds induce cancer. *Int. J. Cancer* **27**, 471–474 [CrossRef Medline](#)
3. Mirvish, S. S. (1995) Role of N-nitroso compounds (NOC) and N-nitrosation in etiology of gastric, esophageal, nasopharyngeal and bladder cancer

- and contribution to cancer of known exposures to NOC. *Cancer Lett.* **93**, 17–48 [CrossRef Medline](#)
4. Tricker, A. R. (1997) N-nitroso compounds and man: sources of exposure, endogenous formation and occurrence in body fluids. *Eur. J. Cancer Prev.* **6**, 226–268 [CrossRef Medline](#)
 5. Hecht, S. S. (1998) Biochemistry, biology, and carcinogenicity of tobacco-specific N-nitrosamines. *Chem. Res. Toxicol.* **11**, 559–603 [CrossRef Medline](#)
 6. Lewin, M. H., Bailey, N., Bandaletova, T., Bowman, R., Cross, A. J., Pollock, J., Shuker, D. E., and Bingham, S. A. (2006) Red meat enhances the colonic formation of the DNA adduct O⁶-carboxymethyl guanine: Implications for colorectal cancer. *Cancer Res.* **66**, 1859–1865 [CrossRef Medline](#)
 7. IARC Working Group on the Evaluation of Carcinogenic Risks to Humans (2007) Smokeless tobacco and some tobacco-specific N-nitrosamines. *IARC Monographs on the Evaluation of Carcinogenic Risks to Humans* **89**, 1–592 [Medline](#)
 8. Balbo, S., Johnson, C. S., Kovi, R. C., James-Yi, S. A., O'Sullivan, M. G., Wang, M., Le, C. T., Khariwala, S. S., Upadhyaya, P., and Hecht, S. S. (2014) Carcinogenicity and DNA adduct formation of 4-(methylnitrosamino)-1-(3-pyridyl)-1-butanone and enantiomers of its metabolite 4-(methylnitrosamino)-1-(3-pyridyl)-1-butanol in F-344 rats. *Carcinogenesis* **35**, 2798–2806 [CrossRef Medline](#)
 9. Carlson, E. S., Upadhyaya, P., Villalta, P. W., Ma, B., and Hecht, S. S. (2018) Analysis and identification of 2'-deoxyadenosine-derived adducts in lung and liver DNA of F-344 rats treated with the tobacco-specific carcinogen 4-(methylnitrosamino)-1-(3-pyridyl)-1-butanone and enantiomers of its metabolite 4-(methylnitrosamino)-1-(3-pyridyl)-1-butanol. *Chem. Res. Toxicol.* **31**, 358–370 [CrossRef Medline](#)
 10. Lao, Y., Yu, N., Kassie, F., Villalta, P. W., and Hecht, S. S. (2007) Analysis of pyridyloxobutyl DNA adducts in F344 rats chronically treated with (R)- and (S)-N'-nitrosornicotine. *Chem. Res. Toxicol.* **20**, 246–256 [CrossRef Medline](#)
 11. Lao, Y., Villalta, P. W., Sturla, S. J., Wang, M., and Hecht, S. S. (2006) Quantitation of pyridyloxobutyl DNA adducts of tobacco-specific nitrosamines in rat tissue DNA by high-performance liquid chromatography-electrospray ionization-tandem mass spectrometry. *Chem. Res. Toxicol.* **19**, 674–682 [CrossRef Medline](#)
 12. Peterson, L. A., and Hecht, S. S. (1991) O⁶-Methylguanine is a critical determinant of 4-(methylnitrosamino)-1-(3-pyridyl)-1-butanone tumorigenesis in A/J mouse lung. *Cancer Res.* **51**, 5557–5564 [Medline](#)
 13. Upadhyaya, P., Kalscheuer, S., Hochalter, J. B., Villalta, P. W., and Hecht, S. S. (2008) Quantitation of pyridylhydroxybutyl-DNA adducts in liver and lung of F-344 rats treated with 4-(methylnitrosamino)-1-(3-pyridyl)-1-butanone and enantiomers of its metabolite 4-(methylnitrosamino)-1-(3-pyridyl)-1-butanol. *Chem. Res. Toxicol.* **21**, 1468–1476 [CrossRef Medline](#)
 14. Zhang, S., Wang, M., Villalta, P. W., Lindgren, B. R., Upadhyaya, P., Lao, Y., and Hecht, S. S. (2009) Analysis of pyridyloxobutyl and pyridylhydroxybutyl DNA adducts in extrahepatic tissues of F344 rats treated chronically with 4-(methylnitrosamino)-1-(3-pyridyl)-1-butanone and enantiomers of 4-(methylnitrosamino)-1-(3-pyridyl)-1-butanol. *Chem. Res. Toxicol.* **22**, 926–936 [CrossRef Medline](#)
 15. Du, H., Leng, J., Wang, P., Li, L., and Wang, Y. (2018) Impact of tobacco-specific nitrosamine-derived DNA adducts on the efficiency and fidelity of DNA replication in human cells. *J. Biol. Chem.* **293**, 11100–11108 [CrossRef Medline](#)
 16. Harrison, K. L., Fairhurst, N., Challis, B. C., and Shuker, D. E. (1997) Synthesis, characterization, and immunochemical detection of O⁶-(carboxymethyl)-2'-deoxyguanosine: a DNA adduct formed by nitrosated glycine derivatives. *Chem. Res. Toxicol.* **10**, 652–659 [CrossRef Medline](#)
 17. Harrison, K. L., Jukes, R., Cooper, D. P., and Shuker, D. E. (1999) Detection of concomitant formation of O⁶-carboxymethyl- and O⁶-methyl-2'-deoxyguanosine in DNA exposed to nitrosated glycine derivatives using a combined immunoaffinity/HPLC method. *Chem. Res. Toxicol.* **12**, 106–111 [CrossRef Medline](#)
 18. Busby, W. F., Jr, Shuker, D. E., Charnley, G., Newberne, P. M., Tannenbaum, S. R., and Wogan, G. N. (1985) Carcinogenicity in rats of the nitrosated bile acid conjugates N-nitrosoglycocholic acid and N-nitrosotaurocholic acid. *Cancer Res.* **45**, 1367–1371 [Medline](#)
 19. Gottschalg, E., Scott, G. B., Burns, P. A., and Shuker, D. E. (2007) Potassium diazoacetate-induced p53 mutations *in vitro* in relation to formation of O⁶-carboxymethyl- and O⁶-methyl-2'-deoxyguanosine DNA adducts: relevance for gastrointestinal cancer. *Carcinogenesis* **28**, 356–362 [Medline](#)
 20. Yang, J., Villalta, P. W., Upadhyaya, P., and Hecht, S. S. (2016) Analysis of O⁶-4-(3-pyridyl)-4-oxobut-1-yl-2'-deoxyguanosine and other DNA adducts in rats treated with enantiomeric or racemic N'-nitrosornicotine. *Chem. Res. Toxicol.* **29**, 87–95 [CrossRef Medline](#)
 21. Leng, J., and Wang, Y. (2017) Liquid chromatography-tandem mass spectrometry for the quantification of tobacco-specific nitrosamine-induced DNA adducts in mammalian cells. *Anal. Chem.* **89**, 9124–9130 [CrossRef Medline](#)
 22. Li, L., Perdigo, J., Pegg, A. E., Lao, Y., Hecht, S. S., Lindgren, B. R., Reardon, J. T., Sancar, A., Wattenberg, E. V., and Peterson, L. A. (2009) The influence of repair pathways on the cytotoxicity and mutagenicity induced by the pyridyloxobutylation pathway of tobacco-specific nitrosamines. *Chem. Res. Toxicol.* **22**, 1464–1472 [CrossRef Medline](#)
 23. Wang, J., and Wang, Y. (2009) Chemical synthesis of oligodeoxyribonucleotides containing N³- and O⁴-carboxymethylthymine and their formation in DNA. *Nucleic Acids Res.* **37**, 336–345 [CrossRef Medline](#)
 24. Wang, J., and Wang, Y. (2010) Synthesis and characterization of oligodeoxyribonucleotides containing a site-specifically incorporated N⁶-carboxymethyl-2'-deoxyadenosine or N⁴-carboxymethyl-2'-deoxycytidine. *Nucleic Acids Res.* **38**, 6774–6784 [CrossRef Medline](#)
 25. Yu, Y., Wang, J., Wang, P., and Wang, Y. (2016) Quantification of azaserine-induced carboxymethylated and methylated DNA lesions in cells by nanoflow liquid chromatography-nano-electrospray ionization tandem mass spectrometry coupled with the stable isotope-dilution method. *Anal. Chem.* **88**, 8036–8042 [CrossRef Medline](#)
 26. Sedgwick, B. (2004) Repairing DNA-methylation damage. *Nat. Rev. Mol. Cell Biol.* **5**, 148–157 [CrossRef Medline](#)
 27. Shrivastav, N., Li, D., and Essigmann, J. M. (2010) Chemical biology of mutagenesis and DNA repair: cellular responses to DNA alkylation. *Carcinogenesis* **31**, 59–70 [CrossRef Medline](#)
 28. Swann, P. F. (1990) Why do O⁶-alkylguanine and O⁴-alkylthymine miscode: the relationship between the structure of DNA containing O⁶-alkylguanine and O⁴-alkylthymine and the mutagenic properties of these bases. *Mutat. Res.* **233**, 81–94 [CrossRef Medline](#)
 29. Meikrantz, W., Bergom, M. A., Memisoglu, A., and Samson, L. (1998) O⁶-Alkylguanine DNA lesions trigger apoptosis. *Carcinogenesis* **19**, 369–372 [CrossRef Medline](#)
 30. Wang, P., and Wang, Y. (2018) Cytotoxic and mutagenic properties of O⁶-alkyl-2'-deoxyguanosine lesions in *Escherichia coli* cells. *J. Biol. Chem.* **293**, 15033–15042 [CrossRef Medline](#)
 31. Peterson, L. A., Thomson, N. M., Crankshaw, D. L., Donaldson, E. E., and Kenney, P. J. (2001) Interactions between methylating and pyridyloxobutylating agents in A/J mouse lungs: implications for 4-(methylnitrosamino)-1-(3-pyridyl)-1-butanone-induced lung tumorigenesis. *Cancer Res.* **61**, 5757–5763 [Medline](#)
 32. Urban, A. M., Upadhyaya, P., Cao, Q., and Peterson, L. A. (2012) Formation and repair of pyridyloxobutyl DNA adducts and their relationship to tumor yield in A/J mice. *Chem. Res. Toxicol.* **25**, 2167–2178 [CrossRef Medline](#)
 33. Ronai, Z. A., Gradia, S., Peterson, L. A., and Hecht, S. S. (1993) G to A transitions and G to T transversions in codon 12 of the Ki-ras oncogene isolated from mouse lung tumors induced by 4-(methylnitrosamino)-1-(3-pyridyl)-1-butanone (NNK) and related DNA methylating and pyridyloxobutylating agents. *Carcinogenesis* **14**, 2419–2422 [CrossRef Medline](#)
 34. Pauly, G. T., Peterson, L. A., and Moschel, R. C. (2002) Mutagenesis by O⁶-4-oxo-4-(3-pyridyl)butyl guanine in *Escherichia coli* and human cells. *Chem. Res. Toxicol.* **15**, 165–169 [CrossRef Medline](#)
 35. Choi, J.-Y., Chowdhury, G., Zang, H., Angel, K. C., Vu, C. C., Peterson, L. A., and Guengerich, F. P. (2006) Translesion synthesis across O⁶-alkylguanine DNA adducts by recombinant human DNA polymerases. *J. Biol. Chem.* **281**, 38244–38256 [CrossRef Medline](#)

Replication studies of NOC-induced O⁶-alkylguanine lesions

36. Choi, J.-Y., and Guengerich, F. P. (2008) Kinetic analysis of translesion DNA synthesis opposite bulky N²- and O⁶-alkylguanine DNA adducts by human DNA polymerase REV1. *J. Biol. Chem.* **283**, 23645–23655 [CrossRef Medline](#)
37. Zhang, F., Tsunoda, M., Suzuki, K., Kikuchi, Y., Wilkinson, O., Millington, C. L., Margison, G. P., Williams, D. M., CzarinaMorishita, E., and Také-naka, A. (2013) Structures of DNA duplexes containing O⁶-carboxymethylguanine, a lesion associated with gastrointestinal cancer, reveal a mechanism for inducing pyrimidine transition mutations. *Nucleic Acids Res.* **41**, 5524–5532 [CrossRef Medline](#)
38. Wu, J., Wang, P., Li, L., Williams, N. L., Ji, D., Zahurancik, W. J., You, C., Wang, J., Suo, Z., and Wang, Y. (2017) Replication studies of carboxymethylated DNA lesions in human cells. *Nucleic Acids Res.* **45**, 7276–7284 [CrossRef Medline](#)
39. Wang, P., Amato, N. J., Zhai, Q., and Wang, Y. (2015) Cytotoxic and mutagenic properties of O⁴-alkylthymidine lesions in *Escherichia coli* cells. *Nucleic Acids Res.* **43**, 10795–10803 [CrossRef Medline](#)
40. Zhai, Q., Wang, P., Cai, Q., and Wang, Y. (2014) Syntheses and characterizations of the *in vivo* replicative bypass and mutagenic properties of the minor-groove O²-alkylthymidine lesions. *Nucleic Acids Res.* **42**, 10529–10537 [CrossRef Medline](#)
41. de Groot, P. M., Wu, C. C., Carter, B. W., and Munden, R. F. (2018) The epidemiology of lung cancer. *Trans. Lung Cancer Res.* **7**, 220–233 [CrossRef Medline](#)
42. Jakszyn, P., Bingham, S., Pera, G., Agudo, A., Luben, R., Welch, A., Boeing, H., Del Giudice, G., Palli, D., Saieva, C., Krogh, V., Sacerdote, C., Tumino, R., Panico, S., Berglund, G., *et al.* (2006) Endogenous versus exogenous exposure to N-nitroso compounds and gastric cancer risk in the European Prospective Investigation into Cancer and Nutrition (EPIC-EURGAST) study. *Carcinogenesis* **27**, 1497–1501 [CrossRef Medline](#)
43. Cross, A. J., Pollock, J. R., and Bingham, S. A. (2003) Haem, not protein or inorganic iron, is responsible for endogenous intestinal N-nitrosation arising from red meat. *Cancer Res.* **63**, 2358–2360 [Medline](#)
44. Warren, J. J., Forsberg, L. J., and Beese, L. S. (2006) The structural basis for the mutagenicity of O⁶-methyl-guanine lesions. *Proc. Natl. Acad. Sci. U.S.A.* **103**, 19701–19706 [CrossRef Medline](#)
45. Johnson, S. J., and Beese, L. S. (2004) Structures of mismatch replication errors observed in a DNA polymerase. *Cell* **116**, 803–816 [CrossRef Medline](#)
46. Janion, C. (2008) Inducible SOS response system of DNA repair and mutagenesis in *Escherichia coli*. *Int. J. Biol. Sci.* **4**, 338–344 [Medline](#)
47. Fuchs, R. P., and Fujii, S. (2013) Translesion DNA synthesis and mutagenesis in prokaryotes. *Cold Spring Harb. Perspect. Biol.* **5**, a012682 [CrossRef Medline](#)
48. Vaisman, A., McDonald, J., and Woodgate, R. (2012) Translesion DNA synthesis. *EcoSal Plus* **5**, doi:10.1128/ecosalplus.7.2.2 [CrossRef Medline](#)
49. Neeley, W. L., Delaney, S., Alekseyev, Y. O., Jarosz, D. F., Delaney, J. C., Walker, G. C., and Essigmann, J. M. (2007) DNA polymerase V allows bypass of toxic guanine oxidation products *in vivo*. *J. Biol. Chem.* **282**, 12741–12748 [CrossRef Medline](#)
50. Yuan, B., Cao, H., Jiang, Y., Hong, H., and Wang, Y. (2008) Efficient and accurate bypass of N²-(1-carboxyethyl)-2'-deoxyguanosine by DinB DNA polymerase *in vitro* and *in vivo*. *Proc. Natl. Acad. Sci. U.S.A.* **105**, 8679–8684 [CrossRef Medline](#)
51. Minko, I. G., Yamanaka, K., Kozekov, I. D., Kozekova, A., Indiani, C., O'Donnell, M. E., Jiang, Q., Goodman, M. F., Rizzo, C. J., and Lloyd, R. S. (2008) Replication bypass of the acrolein-mediated deoxyguanine DNA-peptide cross-links by DNA polymerases of the DinB family. *Chem. Res. Toxicol.* **21**, 1983–1990 [CrossRef Medline](#)
52. Choi, J. Y., Angel, K. C., and Guengerich, F. P. (2006) Translesion synthesis across bulky N²-alkyl guanine DNA adducts by human DNA polymerase κ . *J. Biol. Chem.* **281**, 21062–21072 [CrossRef Medline](#)
53. Yuan, B. F., You, C., Andersen, N., Jiang, Y., Moriya, M., O'Connor, T. R., and Wang, Y. (2011) The roles of DNA polymerases κ and ι in the error-free bypass of N²-carboxyalkyl-2'-deoxyguanosine lesions in mammalian cells. *J. Biol. Chem.* **286**, 17503–17511 [CrossRef Medline](#)
54. Washington, M. T., Minko, I. G., Johnson, R. E., Wolfle, W. T., Harris, T. M., Lloyd, R. S., Prakash, S., and Prakash, L. (2004) Efficient and error-free replication past a minor-groove DNA adduct by the sequential action of human DNA polymerases ι and κ . *Mol. Cell Biol.* **24**, 5687–5693 [CrossRef Medline](#)
55. Li, B. F. L., and Swann, P. F. (1989) Synthesis and characterization of oligodeoxynucleotides containing O⁶-methyl-, O⁶-ethyl-, and O⁶-isopropylguanine. *Biochemistry* **28**, 5779–5786 [CrossRef](#)
56. Smith, C. A., Xu, Y. Z., and Swann, P. F. (1990) Solid-phase synthesis of oligodeoxynucleotides containing O⁶-alkylguanine. *Carcinogenesis* **11**, 811–816 [CrossRef Medline](#)
57. Xu, Y. Z. (2000) Synthesis and characterization of DNA containing O⁶-carboxymethylguanine. *Tetrahedron* **56**, 6075–6081 [CrossRef](#)
58. Wang, L., Spratt, T. E., Pegg, A. E., and Peterson, L. A. (1999) Synthesis of DNA oligonucleotides containing site-specifically incorporated O⁶-4-oxo-4-(3-pyridyl)butyl guanine and their reaction with O⁶-alkylguanine-DNA alkyltransferase. *Chem. Res. Toxicol.* **12**, 127–131 [CrossRef Medline](#)
59. Delaney, J. C., and Essigmann, J. M. (2006) Assays for determining lesion bypass efficiency and mutagenicity of site-specific DNA lesions *in vivo*. *Methods Enzymol.* **408**, 1–15 [CrossRef Medline](#)